Classical Projected Phase Space Density of Billiards and Its Relation to the Quantum Neumann Spectrum

Debabrata Biswas

Theoretical Physics Division, Bhabha Atomic Research Centre, Mumbai 400 085, India
(Received 16 April 2004; published 10 November 2004)

A comparison of classical and quantum evolution usually involves a quasiprobability distribution as a quantum analogue of the classical phase space distribution. In an alternate approach that we adopt here, the classical density is projected on to the configuration space. We show that for billiards, the eigenfunctions of the coarse-grained projected classical evolution operator are identical to a first approximation to the quantum Neumann eigenfunctions. However, even though there exists a correspondence between the respective eigenvalues, their time evolutions differ. This is demonstrated numerically for the stadium and lemon-shaped billiards.

A comparison of classical and quantum dynamics in terms of appropriate evolution operators is of much interest [1–4]. Besides improving our understanding of the statistical properties of quantum spectral fluctuations, these studies are expected to shed light on the effective irreversibility (e.g., relaxation to the invariant density) observed in low-dimensional isolated systems which are otherwise time reversible.

In the probabilistic approach to dynamics, classical time evolution is studied in terms of the propagation of the phase space density, $\rho(p, q)$. The evolution of $\rho(q, p)$ is governed by the Perron-Frobenius (PF) operator, $\mathcal{L}^t$,

$$\mathcal{L}^t \circ \rho(\mathbf{x}) = \int \delta(\mathbf{x} - \mathbf{f}^t(\mathbf{x}'))\rho(\mathbf{x}')d\mathbf{x}', \qquad (1)$$

where $\mathbf{x} = (\mathbf{q}, \mathbf{p})$ is a point in phase space and $\mathbf{f}^t(\mathbf{x})$ is its position at time t. In the Hilbert space of phase space functions, $\mathcal{L}^t$ is unitary [5,6]. The existence of an invariant density, ρ_0, implies $\mathcal{L}^t \circ \rho_0 = \rho_0$. A system is ergodic if the unit eigenvalue is nondegenerate. A knowledge of the spectral decomposition of $\mathcal{L}^t$ allows one to evaluate correlations, averages, and other quantities of interest. For integrable systems, the spectrum of $\mathcal{L}^t$ is discrete, while for mixing systems, there is a continuous spectrum apart from the unit eigenvalue. The exponential decay to the invariant density is connected to the continuous part of the spectrum and reflects in the Fourier transform of time correlations as broad peaks on the real axis [7].

A starting point for the comparison of classical and quantum dynamics is usually a quasiprobability distribution involving the density operator, $\hat{\rho} = |\psi\rangle\langle\psi|$. This enables one to "lift" the quantum state to the phase space. The process is however not unique and depends on the ordering scheme used to arrange the noncommuting operators $(\hat{q}, \hat{p})$ [8,9]. A commonly used quasiprobability distribution is the Husimi function, which is a coherent (most classical) state representation of the quantum density operator. The Husimi propagator is thus a quantum analogue of the Perron-Frobenius operator and the eigen-

states of the two provide a means of comparing quantum and classical evolution.

While the exact Husimi function does not decay to the invariant density, it is found that coarse graining of the phase space leads to a loss of unitarity and the eigenvalues of the coarse-grained classical and quantum propagator have been found to be identical in some cases [3,4].

The primary aim of this Letter is to explore the existence of a correspondence between the classical and quantum spectrum for the class of systems referred to as billiards. However, rather than "lifting" the quantum description to the phase space using a quasiprobability distribution, we shall project the classical density to the configuration space by integrating out the momentum: $\rho(\mathbf{q}) = \int \rho(\mathbf{q}, \mathbf{p})d\mathbf{p}$. While we shall restrict ourselves to billiards here, the essential idea of seeking a quantum-classical correspondence using the projected density instead of the full phase space density is applicable to other systems as well. In the following, we shall show that for billiards, there exists a correspondence between the eigenvalues of the coarse-grained projected classical evolution operator ($\mathcal{L}_P^t$) and the quantum Neumann spectrum, while the respective eigenfunctions are identical to a first approximation. However, the eigenvalues evolve differently with time so that classical and quantum evolution differ [10].

Billiards have relevance in a variety of contexts. The Helmholtz equation describing the quantum billiard problem also describes acoustic waves, modes in microwave cavities, and has relevance in studies on "quantum wells," "quantum corrals," mesoscopic systems, and nanostructured materials.

In a classical billiard, a particle moves freely inside an enclosure and reflects specularly from the boundary. Depending on its shape, billiards exhibit the entire range of behavior observed in other dynamical systems. They also provide a means of coarse graining that is perhaps unique. The dynamics of smooth billiards can be coarse grained by polygonalizing the boundary [12–14].

Rational polygonal billiards are nonergodic and nonmixing. However, the short time dynamics of a polygonalized billiard can approximate that of the smooth billiard [13].

The quantum billiard problem consists of determining the eigenvalues and eigenfunctions of the Helmholtz equation $\nabla^2 \psi(q) + k^2 \psi(q) = 0$ with $\psi(q) = 0$ (Dirichlet) or $\hat{\mathbf{n}}.\nabla \psi = 0$ (Neumann boundary condition; $\hat{\mathbf{n}}$ is the unit normal) on the boundary. Its semiclassical description holds the key to the quantum-classical correspondence. However, since a quantum state (or the quasiprobability distributions constructed out of it) can essentially resolve phase space structures of the size of a Planck cell, polygonalization provides just as much information about the quantum state at the semiclassical level [14,15].

We shall consider a polygonalized billiard as an example of a coarse-grained system. The "unfolded" dynamics of a polygonalized billiard can be viewed locally as a straight line on a singly connected invariant surface consisting of multiple copies of the enclosure glued together appropriately at the edges, each copy denoting a momentum direction that is related to the previous one by the law of reflection at the glued edge (for a figure, see [11,16]). As the magnitude of the momentum (p) and the angle φ that $\mathbf{p}$ makes with (say) the x axis are conserved, it is convenient to treat $\mathbf{p}$ in polar coordinates (p, φ). Transforming from (p_x, p_y) to (p, φ), the $\mathbf{p}$ integration in Eq. (1) simplifies as

$$\int dp_x dp_y \delta(p_x - p_x^{\prime t}(\mathbf{q}', \mathbf{p}')) \delta(p_y - p_y^{\prime t}(\mathbf{q}', \mathbf{p}')) h(\mathbf{q}', \mathbf{p}') = \int d\varphi \, \delta(\varphi - \varphi') h(\mathbf{q}_{\mathbf{u}}', \varphi'; p) = h(\mathbf{q}_{\mathbf{u}}', \varphi; p), \quad (2)$$

where $\mathbf{q}_{\mathbf{u}}$ is a point on the unfolded space, $p_x^{\prime t}(\mathbf{q}', \mathbf{p}')$ ($p_y^{\prime t}$) is the $x(y)$ component of the momentum at time t for the initial phase space coordinate ($\mathbf{q}', \mathbf{p}'$), and

$$h(\mathbf{q}_{\mathbf{u}}', \varphi; p) = \delta(\mathbf{q}_{\mathbf{u}} - \mathbf{q}_{\mathbf{u}}^{\prime t}(\mathbf{q}_{\mathbf{u}}'; \varphi, p)) \rho(\mathbf{q}_{\mathbf{u}}'; \varphi, p). \quad (3)$$

Thus $\mathcal{L}^t \circ \rho = \int d\mathbf{q}_{\mathbf{u}}' \delta(\mathbf{q}_{\mathbf{u}} - \mathbf{q}_{\mathbf{u}}^{\prime t}(\mathbf{q}_{\mathbf{u}}'; \varphi, p)) \rho(\mathbf{q}_{\mathbf{u}}')$. Note that the time evolution of ρ depends on φ through the kernel as $\mathbf{q}_{\mathbf{u}}^{\prime t}$ depends on both the initial position and momentum. Thus $\mathcal{L}^t = \mathcal{L}^t(\varphi)$.

Projection onto to the configuration space requires an integration over the angle φ. The time evolution of the projected density is thus given by:

$$\mathcal{L}_P^t \circ \rho(\mathbf{q}) = \frac{1}{2\pi} \int_0^{2\pi} d\varphi \, \mathcal{L}^t(\varphi) \circ \rho(\mathbf{q})$$

$$= \frac{1}{2\pi} \int d\mathbf{q}_{\mathbf{u}}' d\varphi \, \delta(\mathbf{q}_{\mathbf{u}}$$

$$- \mathbf{q}_{\mathbf{u}}^{\prime t}(\mathbf{q}_{\mathbf{u}}'; p, \varphi)) \rho(\mathbf{q}'). \quad (4)$$

The spectrum of $\mathcal{L}_P^t$ can be studied by evaluating its trace

$$\mathrm{Tr} \mathcal{L}_P^t = \frac{1}{2\pi} \int_0^{2\pi} d\varphi \sum_n e^{\lambda_n(\varphi)t} \quad (5)$$

$$= \frac{1}{2\pi} \int d\mathbf{q}_{\mathbf{u}} \int d\varphi \, \delta(\mathbf{q}_{\mathbf{u}} - \mathbf{q}_{\mathbf{u}}^t(\mathbf{q}_{\mathbf{u}}; p, \varphi)). \quad (6)$$

Note that due to the multiplicative nature of the Perron-Frobenius operator, $\mathcal{L}^t$, its eigenvalues $\Lambda_n(t; \varphi)$ are of the form $e^{\lambda_n(\varphi)t}$. It can be shown that for $t > 0$ [11]

$$\mathrm{Tr} \mathcal{L}_P^t \simeq NC + N \sum_{n=1}^{\infty} g(\sqrt{E_n} l), \quad (7)$$

where $\{E_n\}$ refers to the quantum Neumann spectrum, $l = tv$ where v refers to the velocity, $g(x) = \sqrt{2/(\pi x)} \cos(x - \pi/4)$, N is the maximum number of allowed momentum directions, and $C \simeq 1/N$ is a constant

[17,18]. Since $g(x) \simeq \frac{1}{2\pi} \int_0^{2\pi} e^{ix \sin(\varphi)} d\varphi$ for large x, it follows that for $v = 1$, $\lambda_n(\varphi) = i\sqrt{E_n} \sin(\varphi)$. Thus, the power spectrum of a projected density contains peaks at $\sqrt{E_n}$.

The above correspondence between the classical and quantum spectrum of polygonal billiards arises from a similarity in the traces of $\mathcal{L}_P^t$ and the quantum propagator when expressed in terms of periodic orbits. The correspondence, however, strictly holds for large E_n so long as one uses a delta function kernel in $\mathcal{L}^t$ [11]. For smaller value of E_n, the correspondence exists if the delta function kernel in Eq. (4) is smoothened [11,16]. This effectively results in a coarse graining of the dynamics, and in generic cases, leads to the inclusion of a higher order term in the classical and quantum trace [11,16]. Despite the coarse graining, $\{E_n\}$ in most cases refers to the *approximate* quantum Neumann spectrum as the semiclassical trace formula, which is used in arriving at the correspondence, remains inexact. For integrable polygons such as the rectangle, the correspondence is exact and can be shown directly [11].

Despite the correspondence, quantum time evolution differs from evolution due to $\mathcal{L}_P^t$ as the eigenvalues evolve differently. The quantum Neumann eigenfunctions are however approximate eigenfunctions of $\mathcal{L}_P^t$. This has been established [12] for a quasiclassical adaptation of $\mathcal{L}_P^t$ when the Dirichlet eigenstates are of interest. For the Neumann problem, a similar derivation follows, provided the quasiclassical kernel is replaced by the classical kernel. We shall demonstrate numerically that $\psi_n(\mathbf{q})$ approximates the quantum Neumann eigenfunctions.

For generic polygons, the unit eigenvalue of $\mathcal{L}^t$ is nondegenerate and the corresponding eigenfunction is a constant. This is true as well for the projected operator, $\mathcal{L}_P^t$. Thus $\lambda_0 = 0$. The quantum Neumann problem also has a constant as its ground state eigenfunction and the corresponding eigenenergy $E_0 = 0$.

In order to determine the eigenvalues and eigenfunctions of $\mathcal{L}_P^t$, we shall first evaluate its smoothened kernel

$$K_P(\mathbf{q}, \mathbf{q}', t) = \frac{1}{2\pi} \int d\varphi\, \delta_\epsilon(\mathbf{q} - \mathbf{q}'^t(\varphi))$$
$$= \sum_n \psi_n(\mathbf{q})\psi_n^*(\mathbf{q}')\Lambda_n(t) \qquad (8)$$

as a function of time. Here δ_ϵ is a smoothened delta function and $\psi_n(\mathbf{q})$ are the eigenfunctions of the projected Perron-Frobenius operator, $\mathcal{L}_P^t$. As an example of the smoothened delta function, we consider the hat function, which is zero outside a cell of size ϵ [19]. The φ integration is performed by shooting trajectories from a point $\mathbf{q}'$ at various angles and evaluating the fraction of trajectories in a cell of size ϵ at $\mathbf{q}$ [11]. Since $\lambda_n = i\sqrt{E_n}\sin(\varphi)$, for $\nu = 1$, a Fourier transform of $K_P(\mathbf{q}, \mathbf{q}', t)$ has peaks at $k = \sqrt{E_n}$, the width depending on ϵ and the heights on $\psi_n(\mathbf{q})$. An eigenfunction corresponding to a particular eigenvalue can thus be measured by varying $\mathbf{q}$ and measuring the height of the desired peak.

We now present our numerical results for the stadium and lemon-shaped billiards. The chaotic stadium-shaped billiard that we consider consists of two parallel straight segments of length 2 joined on either end by a semicircle of unit radius. This has been polygonalized using ten segments to approximate the semicircle. Figure 1(a) shows the eigenfunction of $\mathcal{L}_P^t$ corresponding to the first
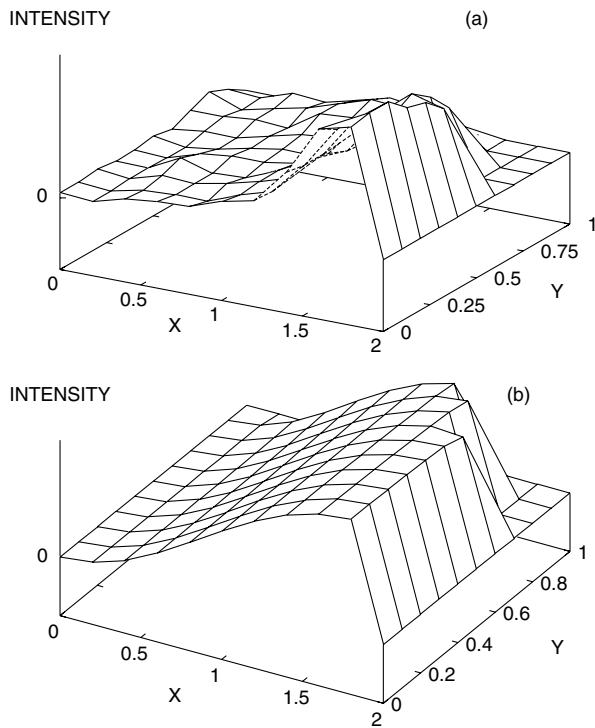
peak at a nonzero k ($k \simeq 0.70$) in the power spectrum of (the smoothened) kernel $K_P(\mathbf{q}, \mathbf{q}, t)$ for the polygonalized stadium. Only the first quadrant is shown due to the reflection symmetry of the system. Note that we have plotted the intensities as the peak heights are proportional to $|\psi_n(q)|^2$. Figure 1(b) shows the corresponding quantum Neumann eigenfunction of the smooth stadium at $k \simeq 0.87$ found using the boundary integral technique. Such a correspondence is seen to exist for other states as well.

We consider next a lemon-shaped enclosure constructed by the intersection of two circles of radius 2.5 centered at $(2, 0)$ and $(-2, 0)$, respectively. Each arc is approximated by seven segments. Figure 2 shows a comparison similar to Fig. 1 for this enclosure for the third peak in the power spectrum of K_P at $k \simeq 3.08$. The agreement with the exact quantum eigenfunction ($k \simeq 3.51$) of the smooth lemon-shaped billiard is again reasonable.

We have thus seen that there is a correspondence, albeit approximate, between the eigenstates of the quantum and projected classical evolution operators. The theoretical basis (see also [11]) clearly indicates that the eigenstates obtained using this method are at best "semiclassical" in nature. In cases where the corrections are zero (rectangle or equilateral billiard), the quantum Neumann eigen-
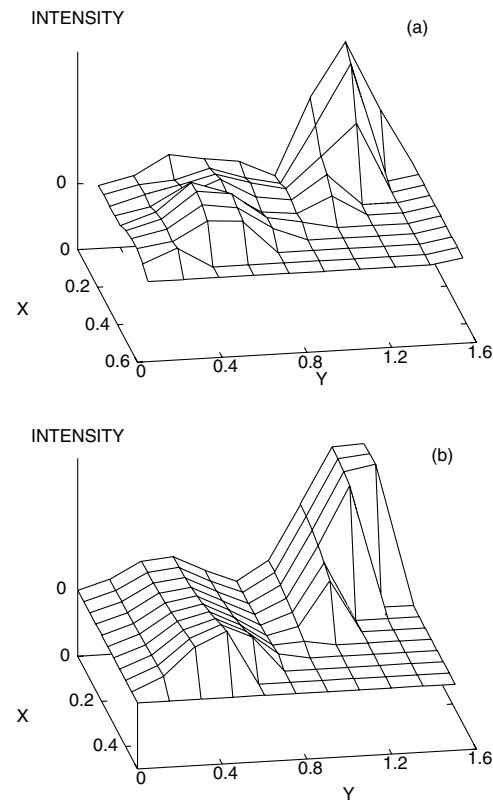

FIG. 1. (a) An eigenfunction of $\mathcal{L}_P^t$ corresponding to the first nonzero eigenvalue of the polygonalized stadium. It is symmetric in Y (Neumann) and antisymmetric in X (Dirichlet). (b) Its quantum counterpart in the smooth stadium.

FIG. 2. (a) An eigenfunction of $\mathcal{L}_P^t$ corresponding to the third nonzero eigenvalue of the polygonalized lemon-shaped billiard. It is symmetric in X and antisymmetric in Y. (b) Its quantum counterpart in the smooth lemon with $k \simeq 3.51$.
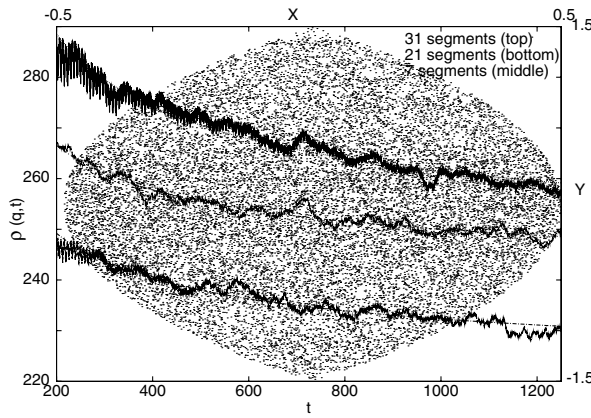
FIG. 3. The time evolution of the locally space and time averaged configuration space density, $\rho(\mathbf{q}, \mathbf{t})$, in a lemon-shaped billiard with different degrees of polygonalization. The number of linear segments approximating each arc is shown in the figure. The point $\mathbf{q}$ is different in each case. The background shows the density at $t \simeq 1250$ for the 31 segment case.

states are identical to the eigenstates of $\mathcal{L}_P$, and the smoothening parameter ϵ can be made small. In general, at higher energies, the peaks in the Fourier transform of $K_P(\mathbf{q}, \mathbf{q}', t)$ are generally harder to resolve as the density of eigenvalues increases with k. Thus, measuring projected eigenfunctions using trajectories becomes harder.

There are basic differences in the interpretations of the quantum and projected classical eigenstates. Each quantum eigenfunction is associated with a density that is invariant in time while only the constant eigenfunction of $\mathcal{L}_P^t$ qualifies as a configuration space density and is invariant. All other densities, $\rho(\mathbf{q})$, decay to the invariant density on evolving with $\mathcal{L}_P^t$. The eigenvalues of $\mathcal{L}_P^t$ thus form a decay spectrum. As an example of the decay to the uniform density in polygonalized billiards, we present in Fig. 3 the evolution of an initially localized projected phase space density, locally averaged in space and time, for three different versions of the polygonalized lemon-shaped billiard considered above. The time evolution of a projected density can be expressed in terms of the eigenstates of $\mathcal{L}_P^t$ as

$$\rho(\mathbf{q}, t) \simeq \rho_{av} + \frac{1}{t^{1/2}} \sum_{n=1}^{\infty} c_n \psi_n(\mathbf{q}) \cos(\sqrt{E_n} t - \pi/4) \quad (9)$$

for t sufficiently large. The coefficients, $\{c_n\}$, apart from some factors, depend on $\int \psi_n(\mathbf{q})\rho(\mathbf{q}, 0)d\mathbf{q}$. The approach to the uniform density, ρ_{av}, is highly oscillatory and the overall decay rate may differ from $t^{-1/2}$ due to the sum of oscillatory terms. We have estimated the overall decay by locally averaging $\rho(\mathbf{q}, t)$ over time. For each of the three cases in Fig. 3, the best fit of $a + b/t^{1/2}$ is also shown. These results testify that there is a decay to the uniform density in polygonalized enclosures.

A discussion on coarse graining is important to understand the significance of the result. There are two levels at which this has been carried out. Polygonalization enables us to connect the quantum and classical eigenvalues analytically. As the number of segments can be increased to approximate the smooth billiard arbitrarily well, it might be expected that the eigenvalues and eigenfunctions converge to those of the smooth billiard in both the quantum and classical case. We have verified this numerically for a few eigenstates of stadium and lemon billiards. Thus coarse graining via polygonalization might be unimportant for observing the correspondence. The second and more significant coarse graining of the dynamics is related to the smoothening of the delta function kernel. This enables us to connect the classical and quantum eigenvalues even for smaller values of λ_n and is hence indispensable.

Finally, it is worth noting that the determination of exact eigenstates of the Perron-Frobenius operator is generally nontrivial while quantum states are easier to determine. The usefulness of the results presented here thus lies in using quantum states to evolve classical configuration space densities.

[1] M. Sano, Phys. Rev. E **59**, R3795 (1999).
[2] D. Braun, Chaos **9**, 730 (1999).
[3] C. Manderfeld, J. Weber, and F. Haake, J. Phys. A **34**, 9893 (2001).
[4] S. Nonnenmacher, Nonlinearity **16**, 1685 (2003).
[5] A. Lasota and M. MacKey, *Chaos, Fractals, and Noise; Stochastic Aspects of Dynamics* (Springer-Verlag, Berlin, 1994).
[6] P. Gaspard, *Chaos, Scattering and Statistical Mechanics* (Cambridge University Press, Cambridge, England, 1998).
[7] M. Pollicott, Inventiones Mathematicae **81**, 413 (1985); D. Ruelle, Phys. Rev. Lett. **56**, 405 (1986).
[8] R. R. Puri, *Mathematical Methods of Quantum Optics* (Springer, Berlin, 2001).
[9] W. Zhang, D. Feng, and R. Gilmore, Rev. Mod. Phys. **62**, 867 (1990).
[10] For a quasiclassical adaptation of $\mathcal{L}_P^t$ for the quantum Dirichlet spectrum, see [11,12]. Note that $\mathcal{L}_P^t$ is not interpreted in [11,12] as the evolution operator for a projected classical density.
[11] D. Biswas, Phys. Rev. E **63**, 016213 (2001).
[12] D. Biswas, Phys. Rev. E **67**, 026208 (2003).
[13] J. L. Vega, T. Uzer, and J. Ford, Phys. Rev. E **48**, 3414 (1993).
[14] D. Biswas, Phys. Rev. E **61**, 5073 (2000).
[15] The degree of polygonalization depends on the de Broglie wavelength, λ; see [14].
[16] D. Biswas, Phys. Rev. E **61**, 5129 (2000).
[17] D. Biswas and S. Sinha, Phys. Rev. Lett. **70**, 916 (1993).
[18] D. Biswas, Phys. Rev. E **54**, R1044 (1996).
[19] The smoothening parameter $\epsilon \sim \mathcal{O}(1/k_{max})$ where k_{max} is the largest eigenvalue of interest [11].